Article:
Liu, M, Gao, C, Zhang, X et al. (4 more authors) (2022) Transformations from cone responses to opponent color spaces. Color Research & Application, 47 (2). pp. 243-251. ISSN 0361-2317

https://doi.org/10.1002/col.22732

Transformations from cone responses to opponent color spaces

Meiyue Liu[1], Cheng Gao[1], Xiaohui Zhang[1], Manuel Melgosa[2], Kaida Xiao[1,3], Daniel Vázquez[4] and Changjun Li[1]

[1] School of Computer and Software Engineering, University of Science and Technology Liaoning, Anshan, China
[2] Department of Optics, University of Granada, Granada, Spain
[3] School of Design, University of Leeds, Leeds, UK
[4] Faculty of Optics and Optometry, Complutense University of Madrid, Madrid, Spain

Correspondence
Changjun Li, School of Computer and Software Engineering, University of Science and Technology Liaoning, Anshan, 114051, China. Email: cjliustl@sina.com

ABSTRACT
We have described a number of transformations by mapping the cone signal vector C, formed by LMS, to opponent space O, formed by achromatic signal O_A, red-green signal O_{rg}, and yellow-blue signal O_{yb}. Two new transformations, Γ_{op1} and Γ_{op2}, are proposed, based on the CIE 2006 spectral luminous efficiency function, $V_F(\lambda)$, and Hurvich's opponent spectral red-green and yellow-blue responses, $H_{rg}(\lambda)$ and $H_{yb}(\lambda)$, without and with constraints, respectively. Γ_{op1} is better than Γ_{op2} in terms of best fit of $H_{rg}(\lambda)$ and $H_{yb}(\lambda)$, and both transformations improved previously proposed ones. Finally, we discuss the *neutral conditions* in cone space using each of the new and some of the extant transformations, as well as choosing scaling factors so that the *neutral conditions* in cone space are satisfied.

KEYWORDS
Cone fundamentals, opponent color space, opponent spectral responses

INTRODUCTION

In 2006, the International Commission on Illumination (CIE) recommended 2 and 10 degrees cone fundamental responses[1-2]. Figure 1 shows the CIE 2006 2-degree $\bar{l}(\lambda)$ (red), $\bar{m}(\lambda)$ (green) and $\bar{s}(\lambda)$ (blue) cone fundamental spectral responses after normalization (i.e. when each of the responses has a unity peak). For a given stimulus with spectral radiance $\varphi(\lambda)$, cone response signals L, M and S are computed from cone fundamental responses using the following equation:

$$\begin{cases} L = \int_a^b \varphi(\lambda)\bar{l}(\lambda)d\lambda \\ M = \int_a^b \varphi(\lambda)\bar{m}(\lambda)d\lambda \\ S = \int_a^b \varphi(\lambda)\bar{s}(\lambda)d\lambda \end{cases} \tag{1}$$

where a and b are the lower and upper limits, respectively, of the visible range. Achieving cone response signals L, M and S for the spectral radiance $\varphi(\lambda)$ of a certain stimulus is the first stage for all two-step vision theories. The second stage is to transfer cone signals to an opponent color space, i.e. an achromatic signal, O_A, and two opponent chromatic signals, O_{rg} (red-green) and O_{yb} (yellow-blue). If we let the Γ transform be a 3-by-3 matrix, the second stage can be described as a matrix and vector multiplication:

$$\mathrm{O} = \Gamma\mathrm{C} \tag{2}$$

where vector C is formed by cone response signals, vector O is formed by signals in opponent color space, and the superscript T means transpose:

$$C = (L \quad M \quad S)^T \tag{3}$$

and

$$O = (O_A \quad O_{rg} \quad O_{yb})^T. \tag{4}$$

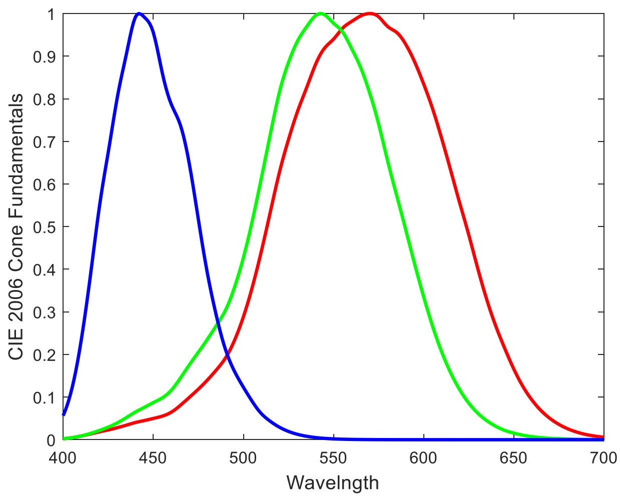

Figure 1. CIE 2006 2-degree cone fundamentals $\bar{l}(\lambda)$ (red), $\bar{m}(\lambda)$ (green) and $\bar{s}(\lambda)$ (blue), ranging from 400nm to 700nm.

Different Γ transforms have been proposed in previous studies. For example, from Figure 3 in the paper by Stockman and Brainard[3], we have

$$\Gamma_{SB} = \begin{pmatrix} 1 & 1 & 0 \\ 1 & -1 & 0 \\ 1 & 1 & -1 \end{pmatrix}. \tag{5}$$

From Figure 1.4 in the book by Hunt and Pointer[4] we have

$$\Gamma_{HP} = \begin{pmatrix} 2 & 1 & 1/20 \\ 1 & -1 & 0 \\ 1 & 1 & -2 \end{pmatrix}. \tag{6}$$

From Figure 1(8.3.4), p. 647, in the book by Wyszecki and Stiles[5], we have

$$\Gamma_{WS} = \begin{pmatrix} 1 & 1 & 0 \\ 1 & -1 & 0 \\ 1 & 0 & -1 \end{pmatrix}. \tag{7}$$

In 2020, Wuerger et al.[6] proposed

$$\Gamma_W = \begin{pmatrix} 1 & 1 & 0 \\ 1 & -\frac{L_0}{M_0} & 0 \\ 1 & 1 & -\frac{L_0+M_0}{S_0} \end{pmatrix}, \tag{8}$$

where L_0, M_0 and S_0 are the cone response signals for the neutral background under the given illuminant.

In 2021, from similarities in wavelength peaks in 16 studies of cone responses and 15 studies of opponent chromatic responses, Pridmore[7] proposed the following matrix for obtaining the two color opponent signals, O_{rg} and O_{yb}, from vector C in Eq. 3:

$$\Gamma_P = \begin{pmatrix} 1 & -1 & 1 \\ 1 & 0 & -1 \end{pmatrix} \tag{9}$$

Recently, the CIE has set up its Technical Committee (TC) 1-98, “a roadmap towards basing CIE colorimetry on cone fundamentals,” for studying the establishment of a new colorimetry based on cone response signals. As we have learned from current CIE colorimetry, developed from CIE color-matching functions, an opponent color space (e.g. the CIELAB color space) is a key tool for the theoretical and practical applications of color science[8]. The currently unsolved problem is which transform should be used for transforming cone response signals to opponent color signals. In this paper, we want to evaluate the above-mentioned transforms in terms of their fitting both the CIE spectral luminous efficiency function and the opponent chromatic spectral response signals reported by Hurvich[9]. Figure 2 shows Hurvich’s opponent signals: $H_{rg}(\lambda)$ (solid curve) is the red-green spectral response and $H_{yb}(\lambda)$ (dotted curve) is the yellow-blue spectral response. More specifically, by using these valuable experimental data sets as references, in the current paper we will develop two new Γ transforms (see Eq. (2)), and discuss the *neutral conditions* in cone space for using each of the transforms defined by Eqs. (5)-(9) and the new transforms. We will also discuss how to choose scaling factors so that the *neutral conditions* in cone space are satisfied.

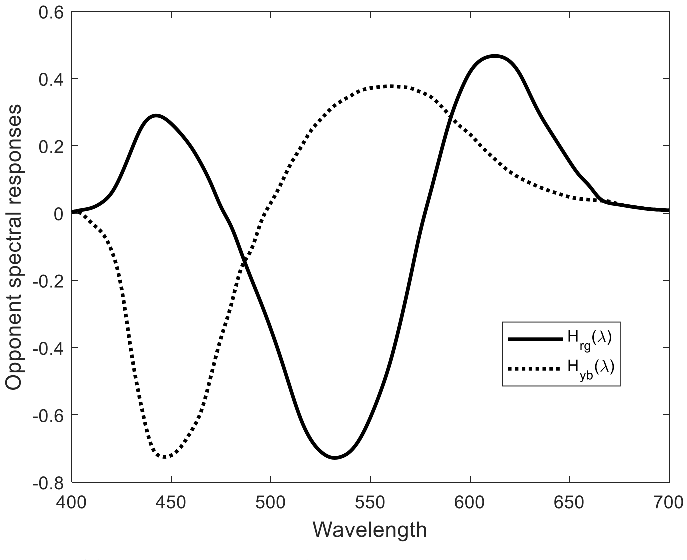

Figure 2. Opponent red-green $H_{rg}(\lambda)$ and yellow-blue $H_{yb}(\lambda)$ spectral responses redrawn from Hurvich (1981).

NEW TRANSFORMS

Firstly, from Eq. (2), if we let

$$C = c(\lambda) = (\bar{l}(\lambda) \quad \bar{m}(\lambda) \quad \bar{s}(\lambda) \ )^T, \tag{10}$$

the achromatic and opponent O signals are also dependent on the wavelength. Hence, we will let

$$O = o(\lambda) = (o_A(\lambda) \quad o_{rg}(\lambda) \quad o_{yb}(\lambda))^T. \tag{11}$$

Since O_A is the achromatic signal in the opponent color space, we can expect $o_A(\lambda)$ to be close to the spectral luminous function. Several spectral luminous efficiency functions are available, including the Judd extension[10], the CIE 1931 color-matching function $\bar{y}(\lambda)$, and the $V_F(\lambda)$, based on CIE 2006 2-degree cone fundamentals[1-2]. Since this paper focuses on cone fundamentals, we have chosen the $V_F(\lambda)$ function as our reference.

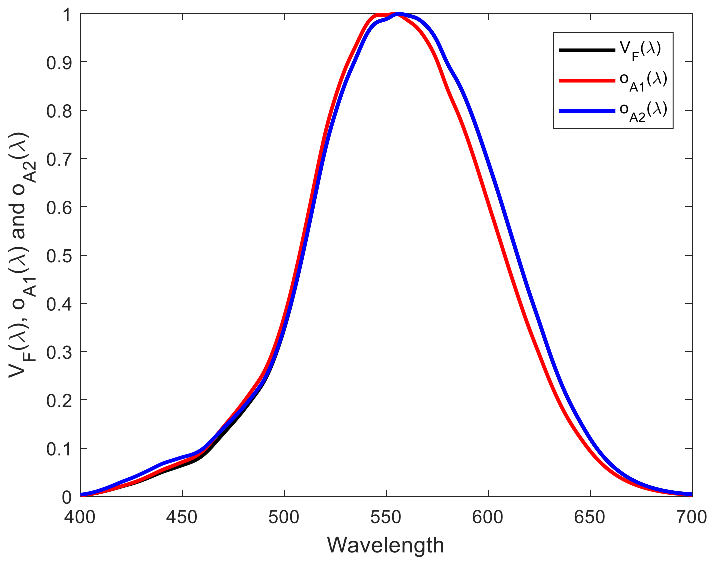

Figure 3. The CIE spectral luminous efficiency function $V_F(\lambda)$ (black), plus two normalized (unity peak) functions, $o_{A1}(\lambda)$ (red) and $o_{A2}(\lambda)$ (blue) (see main text), ranging from 400nm to 700nm.

Let $o_{A1}(\lambda) = o_A(\lambda)$, obtained using the transforms defined by Eqs. (5), (7), or (8), and $o_{A2}(\lambda) = o_A(\lambda)$, obtained using the transform defined by Eq. (6). Figure 3 shows $V_F(\lambda)$ (black), as well as the normalized (unity peak) $o_{A1}(\lambda)$ (red) and $o_{A2}(\lambda)$ (blue) functions. As we can see, the normalized $o_{A1}(\lambda)$ (red) and $o_{A2}(\lambda)$ (blue) functions are quite close to $V_F(\lambda)$ (black). In particular, $V_F(\lambda)$ (black) and $o_{A2}(\lambda)$ (blue) nearly overlap for wavelengths greater than 475nm. In fact, from CIE[1-2], we have:

$$V_F(\lambda) = 0.68990272\bar{l}(\lambda) + 0.34832189\bar{m}(\lambda). \tag{12}$$

Hence, if the desired Γ transform (Eq. (2)) has the general form of

$$\Gamma = \begin{pmatrix} t_{11} & t_{12} & t_{13} \\ t_{21} & t_{22} & t_{23} \\ t_{31} & t_{32} & t_{33} \end{pmatrix}, \tag{13}$$

then the best choice for the first row of Γ is:

$$(t_{11} \quad t_{12} \quad t_{13}) = (0.68990272 \quad 0.34832189 \quad 0)\ . \tag{14}$$

Next, we will consider the two opponent red-green, O_{rg}, and yellow-blue, O_{yb}, signals. When we consider that $C = c(\lambda)$, defined by Eq (10), we can expect that $o_{rg}(\lambda)$ and $o_{yb}(\lambda)$ (see Eq. (11)) will be close to the red-green $H_{rg}(\lambda)$ and yellow-blue $H_{yb}(\lambda)$ spectral responses (see Fig. 2), respectively.

Let us consider the red-green channel first. From Eqs. (5)-(8) and (13), the first case (denominated RG-Case1) for the transform is

$$(t_{21} \quad t_{22} \quad t_{23}) = (1 \quad -\mathrm{x} \quad 0). \tag{15}$$

When $\mathrm{x} = 1$, the situation is that of Eqs. (5)-(7), and when $\mathrm{x} = \frac{L_0}{M_0}$, the situation is that of Eq. (8). We computed the best x so that $o_{rg}(\lambda)$ is closest to $H_{rg}(\lambda)$, and it was found that $x = 1.50273093$.

From Eq. (9) (denominated RG-Case2) we have

$$(t_{21} \quad t_{22} \quad t_{23}) = (1 \quad -1 \quad 1). \tag{16}$$

In addition, we computed the best $(t_{21} \quad t_{22} \quad t_{23})$ so that $o_{rg}(\lambda)$ is closest to $H_{rg}(\lambda)$ (denominated RG-Case3), resulting in a least squares problem[11] with the following solution:

$$(t_{21} \quad t_{22} \quad t_{23}) = (1.19285019 \quad -1.74043682 \quad 0.35227109). \tag{17}$$

The fourth case (denominated RG-Case4) was to find the best $(t_{21} \quad t_{22} \quad t_{23})$ so that $o_{rg}(\lambda)$ is closest to $H_{rg}(\lambda)$ with constraint by the following Eq. (18):

$$t_{21} + t_{22} + t_{23} = 0, \tag{18}$$

resulting in a constrained least squares problem[11] with the solution:

$$(t_{21} \quad t_{22} \quad t_{23}) = (1.20150523 \quad -1.67794634 \quad 0.47644111). \tag{19}$$

Note that the above constraint (Eq. (18)) and the constraint considered later (Eq. (25)) are for the Γ transform (see Eq. (2)), mapping neutral in *LMS* cone space to neutral in opponent color space, with the neutral signals L_0, M_0, and S_0 satisfying $S_0 = L_0 = M_0$. This is widely used in the color and vision community[4-5] and will be further considered in the next section.

Figure 4 shows Hurvich's opponent red-green function $H_{rg}(\lambda)$ (black), and the red-green spectral responses achieved from RG-Case1 (red), RG-Case2 (blue), RG-Case3 (magenta), and RG-Case4 (yellow). It can be clearly seen that their order of closeness to the black curve is: magenta, yellow, red, and blue. Hence, RG-Case3 is the best, followed by RG-Case4, RG-Case1, and RG-Case2.

We can measure the closeness between $H_{rg}(\lambda)$ and the red-green spectral responses achieved by each of our four above cases by using different tools, such as the *root mean square error* (*RMSE*)[12] or the *goodness of fit coefficient* (*GFC*) used in previous literature[13]. Let q be a vector with n elements, and p an approximation to q, also with n elements. *RMSE* and *GFC* between q and p are defined by:

$$RMSE = \sqrt{\frac{1}{n}\sum_{i=1}^{n}(q_i - p_i)^2} \tag{20}$$

and

$$GFC = q^T p / (||q||_2 ||p||_2) \text{ with } ||q||_2 = \sqrt{\sum_{i=1}^{n}(q_i)^2}\ ,\ ||p||_2 = \sqrt{\sum_{i=1}^{n}(p_i)^2} \quad . \tag{21}$$

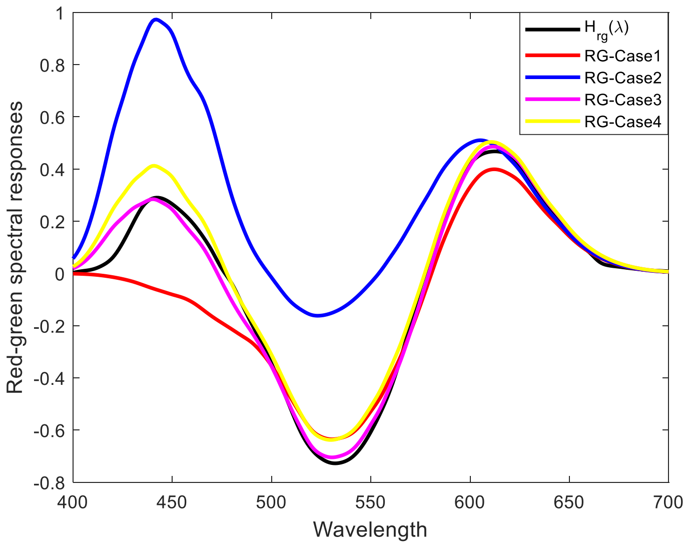

Figure 4. Hurvich's opponent red-green $H_{rg}(\lambda)$ function (black), together with the red-green spectral responses from RG-Case1, RG-Case2, RG-Case3 and RG-Case4, respectively (see main text).

Thus, if $q = p$, *RMSE*=0. The closer p and q are, the smaller *RMSE* is. For *GFC*, it is always equal or smaller than 1, and the closer to 1 the better the agreement between p and q. Table 1 lists the *RMSE* (column 2) and *GFC* (column 3) values between Hurvich's opponent red-green function $H_{rg}(\lambda)$ and the spectral responses achieved for each of our four cases. It can be seen from both measurements that the four cases, ordered from best to worst, are RG-Case3, RG-Case4, RG-Case1, and RG-Case2, which is in agreement with the results shown in Figure 4.

Note that from Eq. (15) with $\mathrm{x} = 1.50273093$ for RG-Case1, we cannot expect the transforms Γ_{SB}, Γ_{HP}, Γ_{WS} and Γ_{W} (Eqs. (5)-(8)) to perform better than RG-Case3 and RG-Case4, in terms of fitting Hurvich's opponent red-green function, $H_{rg}(\lambda)$. Similarly, RG-Case2, corresponding to the transform Γ_{P} (Eqs. (9) and (16)), is not expected to perform better than RG-Case3 and RG-Case4 in terms of fitting Hurvich's opponent red-green function $H_{rg}(\lambda)$.

Table 1: *RMSE*[12] and *GFC*[13] values between Hurvich's opponent red-green (RG) and yellow-blue (YB) functions and the four corresponding models (Case1-Case4) considered in the current article (see main text).

	RG		**YB**	
	RMSE	*GFC*	*RMSE*	*GFC*
Case1	0.139	0.920	0.800	0.754
Case2	0.391	0.475	0.369	0.907
Case3	**0.047**	**0.991**	**0.075**	**0.971**
Case4	0.085	0.970	0.127	0.914

We next considered the yellow-blue channel, and distinguished four cases as well. The first, denominated YB-Case1, is the following:

$$(t_{31} \quad t_{32} \quad t_{33}) = (1 \quad 1 \quad -\mathrm{y}). \tag{22}$$

When $\text{y} = 1$, $\text{y} = 2$, and $\text{y} = -\frac{L_0+M_0}{S_0}$, we are presented with the situations indicated in previous Eqs. (5), (6) and (8), respectively. The best y value for $o_{yb}(\lambda)$, in order of closeness to $H_{yb}(\lambda)$, is $y = 0.92299502$.

The second case, denominated YB-Case2, is the following:

$$(t_{31} \quad t_{32} \quad t_{33}) = (1 \quad 0 \quad -1). \tag{23}$$

This case was given by Eq. (7) and by Eq. (9) in the recent paper[9] by Pridmore.

The third case, denominated YB-Case3, is to find the best $(t_{31} \quad t_{32} \quad t_{33})$ so that $o_{yb}(\lambda)$ is closest to $H_{yb}(\lambda)$. Again, we must solve a least squares problem[11] and it was found that

$$(t_{31} \quad t_{32} \quad t_{33}) = (0.24289310 \quad 0.13401208 \quad -0.69913752). \tag{24}$$

Finally, in the fourth case, denominated YB-Case4, we computed the best $(t_{31} \quad t_{32} \quad t_{33})$ so that $o_{yb}(\lambda)$ is closest to $H_{yb}(\lambda)$, with the constraint defined by the following Eq. (25):

$$t_{31} + t_{32} + t_{33} = 0. \tag{25}$$

In this last case it was found that

$$(t_{31} \quad t_{32} \quad t_{33}) = (0.25717223 \quad 0.23710911 \quad -0.49428134). \tag{26}$$

As noted above, constraints in Eqs. (18) and (25) allow the Γ transform (see Eq. (2)) to map the neutral in *L*, *M* and *S* space to the neutral in opponent space when the neutral stimulus signals L_0, M_0, and S_0 satisfy $S_0 = L_0 = M_0$.

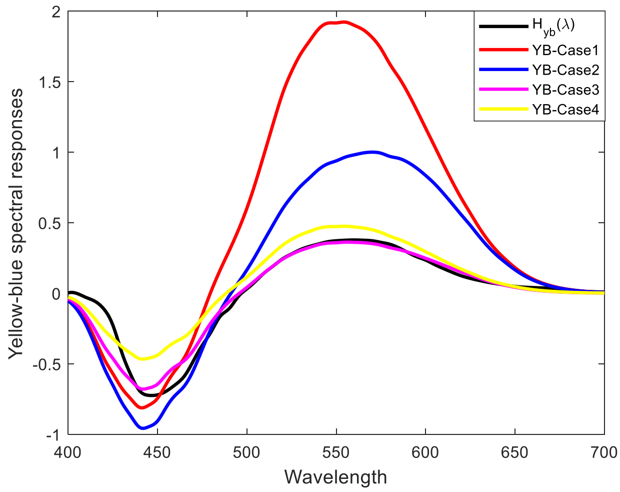

Figure 5. Hurvich's opponent yellow-blue $H_{yb}(\lambda)$ function (black), together with the yellow-blue spectral responses from YB-Case1, YB-Case2, YB-Case3 and YB-Case4, respectively (see main text).

Figure 5 shows Hurvich's opponent yellow-blue spectral function, $H_{yb}(\lambda)$ (black), together with the yellow-blue spectral responses found from YB-Case1 (red), YB-Case2 (blue), YB-Case3 (magenta), and YB-Case4 (yellow). It can be observed that their order of closeness to the black curve is: magenta, yellow, blue, and red. Hence, YB-Case3 is the best, followed by YB-Case4, YB-Case2, and YG-Case1.

Table 1 lists the *RMSE* (column 4) and *GFC* (column 5) values between Hurvich's opponent yellow-blue spectral function $H_{yb}(\lambda)$ and the yellow-blue spectral responses achieved for each of our four cases. It can be seen from both measurements that the best cases are YB-Case3, YB-Case4, YB-Case2, and YB-Case1, in this order, which is consistent with the results observed in Figure 5.

Note that from Eq. (22) with $\text{y} = 0.92299502$ for YB-Case1 we cannot expect transforms Γ_{SB}, Γ_{HP}, and Γ_W (Eqs. (5), (6), (8)) to perform better than for YB-Case3 and YB-Case4 in terms of fitting

Hurvich's opponent yellow-blue function $H_{yb}(\lambda)$. In addition, for YB-Case 2, corresponding to transforms Γ_{WS} and Γ_P, we cannot expect these to have a better performance than for YB-Case3 and YB-Case4 in terms of their fitting Hurvich's opponent yellow-blue function $H_{yb}(\lambda)$.

From all the above discussions, we can conclude that the best transform is based on Eq. (14) for the achromatic signal, Eq. (17) for the red-green signal, and Eq. (24) for the yellow-blue signal. We have named this transform Γ_{op1}, given by:

$$\Gamma_{op1} = \begin{pmatrix} 0.68990272/k_L & 0.34832189/k_M & 0 \\ 1.19285019 & -1.74043682 & 0.35227109 \\ 0.24289310 & 0.13401208 & -0.69913752 \end{pmatrix} . \tag{27}$$

Similarly, we can point out that the second best transform, denominated Γ_{op2}, is the one achieved from Eqs. (14), (19) and (26):

$$\Gamma_{op2} = \begin{pmatrix} 0.68990272/k_L & 0.34832189/k_M & 0 \\ 1.20150523 & -1.67794634 & 0.47644111 \\ 0.25717223 & 0.23710911 & -0.49428134 \end{pmatrix} . \tag{28}$$

Here, k_L, k_M (and k_S) are scaling factors used to compute the cone response signals (see Eq. (1)) that will be considered in the next section (see Eq. (32)). Up to now, we have assumed that $k_L = 1$ and $k_M = 1$ have the best fit for the spectral luminous efficiency function $V_F(\lambda)$.

Note that the above analyses and proposed new transforms used the Hurvich's opponent response functions[9] as reference. Although different sets of opponent response functions are available in the literature (see Table 1 in reference 7), we used Hurvich's opponent response functions because they have been widely used in previous literature, including the recent paper by Pridmore (Figure 2 in reference 7).

DISCUSSIONS AND CONCLUSIONS

In color science, an Γ transform is useful if $O = \Gamma C$ maps the neutral color vector $C_0 = (L_0 \quad M_0 \quad S_0)^T$ to opponent space $O = (O_A \quad O_{rg} \quad O_{yb})^T$ with $O_{rg} = 0$ and $O_{yb} = 0$, which is referred to as a *neutral-to-neutral condition* for the Γ transform considered. It can be verified that the Γ_W transform given by Wuerger et al.[6] (see Eq. (8)) always satisfies this condition. However, for the other transforms described here we can deduce the *neutral condition* in cone space for the neutral color vector $C_0 = (L_0 \quad M_0 \quad S_0)^T$ using this *neutral-to-neutral condition***.**

For example, when using the transform Γ_{SB} defined by Eq. (5), to obtain $O_{rg} = 0$ and $O_{yb} = 0$ we must have the *neutral condition* in cone space:

$$L_0 = M_0 \text{ and } S_0 = 2L_0 = 2M_0 . \tag{29}$$

Note that when using the transforms Γ_{HP}, Γ_{WS}, and Γ_{op2}, defined by Eqs. (6), (7), (28), respectively, the sum of the coefficients in the second and third rows of the matrices is zero, and hence, the *neutral-to-neutral condition* is fulfilled when the neutral color vector C_0 satisfies

$$S_0 = L_0 = M_0 . \tag{30}$$

For the transform Γ_P, defined by Eq. (9), the *neutral-to-neutral condition* is fulfilled if the neutral color vector C_0 satisfies

$$S_0 = L_0 , \quad M_0 = 2L_0 = 2S_0 . \tag{31}$$

To allow the neutral color stimulus to satisfy any of the neutral conditions defined by Eqs. (29)-(31), we must introduce the scaling factors k_L, k_M, and k_S into Eq. (1) to compute the cone response signals LMS, so that

$$\begin{cases} L = k_L \int_a^b \varphi(\lambda)\bar{l}(\lambda)d\lambda \\ M = k_M \int_a^b \varphi(\lambda)\bar{m}(\lambda)d\lambda \\ S = k_S \int_a^b \varphi(\lambda)\bar{s}(\lambda)d\lambda \end{cases} . \tag{32}$$

Let $\varphi_0(\lambda)$ be the spectral radiance for a given neutral stimulus. Then, in order to satisfy the *neutral condition* Eq. (29) in cone space, the scaling factors k_L, $k_{M,}$ and k_S in Eq. (32) are determined by the following Eq. (33) for a given constant c (for example $c = 1$ or 100):

$$k_L \int_a^b \varphi_0(\lambda)\bar{l}(\lambda)d\lambda = k_M \int_a^b \varphi_0(\lambda)\bar{m}(\lambda)d\lambda = c = 0.5k_S \int_a^b \varphi_0(\lambda)\bar{s}(\lambda)d\lambda \tag{33}$$

In order to satisfy the *neutral condition* Eq. (30) in cone space, the scaling factors k_L, k_M, and k_S in Eq. (32) are determined by the following Eq. (34) for a given constant d (for example $d = 1$ or 100):

$$k_L \int_a^b \varphi_0(\lambda)\bar{l}(\lambda)d\lambda = k_M \int_a^b \varphi_0(\lambda)\bar{m}(\lambda)d\lambda = k_S \int_a^b \varphi_0(\lambda)\bar{s}(\lambda)d\lambda = d \tag{34}$$

However, in order to satisfy the *neutral condition* Eq. (31) in cone space, the scaling factors k_L, $k_{M,}$ and k_S in Eq. (32) are determined by the following Eq. (35) for a given constant f (for example $f = 1$ or 100):

$$k_L \int_a^b \varphi_0(\lambda)\bar{l}(\lambda)d\lambda = k_S \int_a^b \varphi_0(\lambda)\bar{s}(\lambda)d\lambda = f = 0.5k_M \int_a^b \varphi_0(\lambda)\bar{m}(\lambda)d\lambda \tag{35}$$

Determining the scaling factors can also be done by using the newly derived transform Γ_{op1}. Let the second and third rows of the transform Γ_{op1} form a matrix A. Then we find the singular value decomposition[11] for A: $A = UDV^T$. Here, the superscript T is the transpose of a matrix, while U and V are 2-by-2 and 3-by-3 orthogonal matrices, respectively. The 2-by-3 matrix D has a special form, given by:

$$D = \begin{pmatrix} \sigma_1 & 0 & 0 \\ 0 & \sigma_2 & 0 \end{pmatrix} \tag{36}$$

where σ_1 and σ_2 are the singular (non-negative) values of the matrix A.

Let v be the third column of the orthogonal matrix V. It can then be verified that $Av = (0 \quad 0)^T$. In fact,

$$v = (0.73201193 \quad 0.57550407 \quad 0.36462803)^T. \tag{37}$$

Hence, the *neutral-to-neutral condition* using the transform Γ_{op1} is satisfied if the neutral color vector C_0 satisfies

$$C_0 = (L_0 \quad M_0 \quad S_0)^T = v \ . \tag{38}$$

In the preceding, we have discussed the *neutral-to-neutral conditions* for several different transforms. A transform is useful if the associated *neutral-to- neutral condition* is satisfied. We have also discussed the *neutral condition* in cone space for each of the transforms considered, and how to choose the scaling factors k_L, $k_{M,}$ and k_S to satisfy these *neutral conditions*. However, different applications may require different *neutral conditions* in cone space, which may limit the choice of transforms. In color science, a widely accepted *neutral condition* is that the three channel response values L_0, M_0, S_0 are equal, resulting in the *neutral condition* in Eq. (30), which ensures that transforms Γ_{HP} (see Eq. (6)), Γ_{WS} (see Eq. (7)), and Γ_{op2} (see Eq. (28) satisfy the *neutral-to-neutral condition*. Among these three transforms, Γ_{op2} is the best in terms of fitting the spectral luminous efficiency function $V_F(\lambda)$ and Hurvich's opponent red-green and yellow-blue responses, $H_{rg}(\lambda)$ and $H_{yb}(\lambda)$.

When the three cone response values L_0, M_0, S_0 do not satisfy any of the *neutral conditions* given by Eqs. (29)-(31) and (38) in cone response space, for a particular application the transform Γ_W (see Eq. (8)) can be used, as this transform does satisfy the *neutral-to-neutral condition* for any *neutral stimulus* in cone space. However, in this case, a better transform can be developed in terms of fitting of the spectral luminous efficiency function $V_F(\lambda)$ and Hurvich's opponent red-green and yellow-blue responses, $H_{rg}(\lambda)$ and $H_{yb}(\lambda)$. In fact, if we let the transform be Γ_{op3}, having 9 parameters (see Eq. (13)), the first row of Γ_{op3} is the same as the first row of Γ_{op1} (or Γ_{op2}), and the second and third rows of Γ_{op3} should satisfy:

$$\begin{pmatrix} H_{rg}(\lambda) \\ H_{yb}(\lambda) \end{pmatrix} = \begin{pmatrix} t_{21} & t_{22} & t_{23} \\ t_{31} & t_{32} & t_{33} \end{pmatrix} c(\lambda) \ , \tag{39}$$

where $c(\lambda)$ is defined by Eq. (10). Furthermore, the second and third rows of Γ_{op3} should satisfy the following constraint:

$$\begin{pmatrix} 0 \\ 0 \end{pmatrix} = \begin{pmatrix} t_{21} & t_{22} & t_{23} \\ t_{31} & t_{32} & t_{33} \end{pmatrix} C_0 \ , \tag{40}$$

where $C_0 = (L_0 \quad M_0 \quad S_0)^T$. Note that condition in Eq. (39) must be satisfied for each wavelength λ, and hence we need to find a least squares solution for Eq. (39). Condition in Eq. (40) is the *neutral-to-neutral condition* for the transform Γ_{op3}, and so the final transform can be obtained by solving a constrained least squares problem[11].

In conclusion, we have examined several transforms (see Eqs. (5)-(9)) mapping the cone signal vector C formed by LMS to opponent color space O (see Eqs. (2)-(4)). We have also derived two new transforms, designated as Γ_{op1} (Eq. (27)) and Γ_{op2} (Eq. (28)), based on the fit of the CIE spectral luminous efficiency function $V_F(\lambda)$ and Hurvich's opponent red-green and yellow-blue responses, $H_{rg}(\lambda)$ and $H_{yb}(\lambda)$, without and with constraints (see Eqs. (18) and (25)), respectively. Γ_{op1} is better than Γ_{op2} in terms of best fit for $H_{rg}(\lambda)$ and $H_{yb}(\lambda)$. Both Γ_{op1} and Γ_{op2} are better than any of the transforms previously proposed (Eqs. (5)-(9)), in terms of fit of Hurvich's red-green and yellow-blue opponent spectral responses. Using the transform Γ_{op1}, the *neutral-to-neutral condition* requires that the scaling factors k_L, k_M, and k_S must be determined so that a *neutral stimulus* in cone space is obtained (Eqs. (37)-(38)). For the transform Γ_{op2}, the *neutral-to-neutral condition* requires that the scaling factors k_L, k_M, and k_S be determined so that the *neutral condition* in Eq. (30) be satisfied. If the *neutral condition* in cone space is different from that defined by Eqs. (30) or (38), an Γ_{op3} transform can be obtained by solving the constrained least squares problem defined by Eqs. (39) and (40).

ACKNOWLEDGEMENTS

This work has been supported by the National Natural Science Foundation of China (Grant numbers: 61575090, 61775169), the Ministry of Science and Innovation of the National Government of Spain (Grant number: PID2019-107816GB-I00/SRA/10.13039/501100011033), the Foundation of Liaoning Province Education Administration, and the graduate education reform, scientific & technological innovation and entrepreneurship project of the University of Science and Technology Liaoning. English assistance from Mr. Donald J, Murphy Mcveigh is acknowledged.

ORCIDs

Changjun Li, https://orcid.org/0000-0002-9942-7690

Manuel Melgosa, https://orcid.org/0000-0002-7226-4190

Data Availability Statement

The data used to support the findings of this study are available from the corresponding author upon request. The data are not publicly available due to privacy restrictions.

REFERENCES

[1] CIE 170-1:2006. Fundamental chromaticity diagram with physiological axes - Part 1. Vienna: CIE; 2006.

[2] CIE 170-2:2015. Fundamental chromaticity diagram with physiological axes - Part 2: Spectral luminous efficiency functions and chromaticity diagrams. Vienna: CIE; 2015.

[3] Stockman A, Brainard DH. Color vision mechanisms. Chapter 11 in OSA Handbook of Optics (3rd edition, Bass M, ed.). McGraw-Hill, New York, pp. 11.1-11.104; 2010.

[4] Hunt RWG, Pointer MR. Measuring Colour, fourth edition. New York: Wiley; 2011.

[5] Wyszecki G, Stiles WS. Color Science: Concepts and Methods, Quantitative Data and Formulae, 2nd edition. New York: Wiley; 2000.

[6] Wuerger S, Ashraf M, Kim M, Martinovic J, Pérez-Ortiz M, Mantiuk RK. Spatio-chromatic contrast sensitivity under mesopic and photopic light levels. *Journal of Vision.* 2020; 20(4): 1–26.

[7] Pridmore RW. A new transformation of cone responses to opponent color responses. *Attention Perception & Psychophysics*. 2021; 83: 1797-1803.

[8] CIE 015:2018. Colorimetry, 4th edition. Vienna : CIE ; 2018.

[9] Hurvich LM. Color vision. Sunderland, Sinauer Associates, Inc. 1981. Figure on p. 62.

[10] CIE 086:1990. CIE 1988 2° spectral luminous efficiency function for photopic vision. Vienna : CIE ; 2090.

[11] Golub GH, Loan CV. Matrix Computation, 4th edition. Baltimore: The Johns Hopkins University Press; 2013.

[12] Carreres-Prieto D, García JT, Cerdán-Cartagena F, Suardiaz-Muro J. Performing calibration of transmittance by single RGB-LED within the visible spectrum. *Sensors*. 2020; 20(12): 3492.

[13] Hernández-Andrés J, Romero J, Lee RL. Colorimetric and spectroradiometric characteristics of narrow-field-of-view clear skylight in Granada, *Journal of the Optical Society of America A*. 2001; 18(2): 412–420.

AUTHORS' BIOGRAPHIES

Meiyue Liu is a graduate student in the Department of Computer Science, University of Science and Technology Liaoning, Anshan, China, where she received her BS in computer science in 2019. Her current research interests are colour and imaging science.

Cheng Gao is a research assistant in the Department of Computer Science, University of Science and Technology Liaoning. He received BS (2015), and MS (2018) degrees in software engineering from this university. His current research interests are spectrum optimization of LED, color appearance modeling, and mesopic luminance computation.

Xiaohui Zhang is a research assistant in the Department of Software Engineering, University of Science and Technology Liaoning. He received BS (2017), and MS (2020) degrees respectively from this university. His current research interests are colour and imaging science.

Manuel Melgosa is full professor in optics and associate editor of this journal. Currently he is the Vice-president of International Affairs of the Lighting Committee of Spain, and the Secretary of the Color Vision and Psychophysics Study Group of the International Color Association. He is also the representative of Spain at CIE Divisions 1 and 8, serving as member of CIE TCs 1-98, 8-14, 8-17, 8-18, JTC 10 (D1/D8) and R1-60. His main research interests are color-difference evaluation and applied colorimetry.

Kaida Xiao is an Associate Professor in the Colour and Imaging Science in the School of Design, University of Leeds, UK. His research interests are 3D colour image reproduction, 3D colour printing, 3D printing facial prostheses, medical image capture and analysis, colour appearance modelling and image quality enhancement.

Daniel Vázquez is professor in the Optics Department of the Universidad Complutense of Madrid since 1988. He received a Ph. D. in architecture by Universidad Politécnica of Madrid. He works in the development of lighting systems applied to several fields such as natural lighting devices, signals, LEDs and solar energy. His current interests include color perception and lighting systems applied to cultural heritage. Among his lat works it can be mentioned studies of Portico de la Gloria gate in Santiago de Compostela, Guernica picture in Reina Sofía Museum of Madrid, and Altamira cave in Cantabria.

Changjun Li is a Professor at the Department of Computer Science, University of Science and Technology Liaoning, Anshan, China. He received his B.Sc. (1979), M.Sc. (1982), Ph.D. (1989) in computational mathematics from Peking University (China), Chinese Academy of Science, and Loughborough University (UK) respectively. His current research interests are chromatic adaptation transform, colour appearance modeling, uniform colour spaces, and computational colour constancy. Currently he is the Chair of CIE JTC10 on CIECAM16.